Materials and Design 186 (2020) 108345

Contents lists available at ScienceDirect

Materials and Design

journal homepage: www.elsevier.com/locate/matdes

Study of the influence of the type of matrix used in carbon-epoxy composites on fatigue delamination under mode III fracture

C. Bertorello [a], J. Viña [a,*], I. Viña [b], A. Argüelles [b]

[a] Department of Materials Science and Metallurgical Engineering, Campus Universitario, 33203 Gijón, Spain
[b] Department of Construction and Manufacturing Engineering, Campus Universitario, 33203 Gijón, Spain

HIGHLIGHTS

- The Longitudinal Half Fixed Beam device is valid for obtaining the values of both static and dynamic energy release rates
- Fracture toughness depends on the matrix but its behaviour varies depending on the type of stress to which it is subjected
- The most typical fractography in mode III-fatigue is formed by cusps with a preferred orientation at 45° and resin beds

GRAPHICAL ABSTRACT

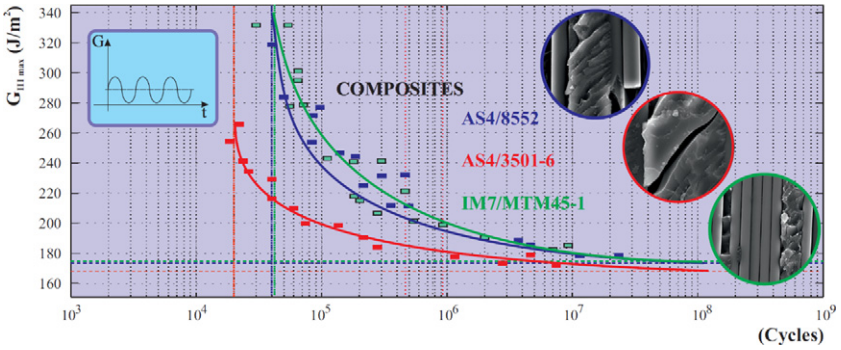

ARTICLE INFO

Article history:
Received 4 October 2019
Received in revised form 7 November 2019
Accepted 8 November 2019
Available online 9 November 2019

Keywords:
Delamination
Fracture
Fatigue
Mode III

ABSTRACT

The fatigue delamination process of three different aeronautical quality composites subject to mode III fracture loading is studied experimentally in this paper with the aim of analysing the effect of the type of matrix used under this fatigue fracture mode. In all cases, the main difference between the composite materials considered in this study is the type of epoxy resin used as the matrix.

The test method used to produce the delamination process under mode III fracture is known as the Longitudinal Half Fixed Beam (LHFB) method, used in previous studies by the authors, which was shown to be a valid method for generating the delamination process in composite sheet materials subject to mode III fatigue loading.

The experimental data from the fatigue tests were treated with a probabilistic model based on the Weibull distribution. This model facilitates the identification of relevant aspects of the fatigue behaviour of these materials, such as the estimation of fatigue strength for periods of time greater than those tested here, as well as the reliability of the results.

The results thus obtained reflect important differences in the fatigue behaviour of the materials under study, the type of matrix being the predominant parameter of the fracture process under mode III loading.

1. Introduction

Composites made from prepregs have a number of drawbacks that are inherent in the manufacturing process used in their consolidation [1]. These materials are highly susceptible to delamination, i.e. to the

* Corresponding author.
E-mail address: jaure@uniovi.es (J. Viña).

https://doi.org/10.1016/j.matdes.2019.108345

formation and growth of interlaminar cracks that propagate between the layers under both static and fatigue conditions. This problem is of major interest to the scientific community as the main result deriving from it is a decrease in stiffness and strength that alters the mechanical behaviour of the material and can significantly reduce its service life.

Although several decades have passed since the scientific community became aware of the importance of the phenomenon of interlaminar fracture [2], it is still a critical parameter that limits the use of laminates in structural components [3–12]. Although most of the aforementioned studies were carried out under static loading, there is a pressing need to obtain reliable and detailed information on the strength of these materials under cyclic fatigue loading [13–16].

This paper focuses on mode III failure, also known as tearing mode failure, when the shear stress moves the lips of the crack in a parallel direction to the crack front, i.e. perpendicular to crack growth [17].

Although this fracture mode has not been as widely studied as modes I and II, a significant number of papers have been published. So far, however, these studies have been carried out under static loading employing different test methods [18,19], as no standard has been developed to date regarding these tests. The best known among existing methods are listed below.

The Split Cantilever Beam (SCB) test [20–23], which uses beam-shaped specimens, is employed in DCB and ENF tests. Although the results thus obtained are acceptable, certain overloads are produced. Szekrényes [22] introduced substantial modifications to the test method, giving rise to the Modified Split Cantilever Beam (MSCB) test. In this case, two loading systems are applied to the test specimen. Another of the test methods, known in the literature as the Edge Crack Torsion (ECT) test [15–32], supposed an evolution in the study of the interlaminar fracture of compounds under mode III fracture and is one of the most widely used methods. It is based on the application of a torque at the embedded end of the specimen. Yoshihara [33] developed the method known as the Four Point Bend End-Notched Flexure (4-ENF_{III}) test. This method may be considered a mode III variation of the 4ENF that uses a large-sized, complex-shaped specimen in which no more than 90% mode III fracture is obtained. Another test method, known as 6ECT, is based on modifications to the conventional ECT method [34,35]. Finally, Davidson and Sediles [36–37] introduced a new test method called the Shear-Torsion-Bending (STB) test that enables testing resistance to delamination under any type of mixed mode loading and which was subsequently modified to study mode III fracture. A test method already employed in previous research by the authors, denominated the Longitudinal Half Fixed Beam (LHFB) test [38–40], was used in the present study. This test was found to be suitable for the characterization of composite materials under this fracture mode.

In this paper, the fatigue delamination process of three different aeronautical quality composites subject to mode III fracture loading is studied experimentally with the fundamental aim of analysing the effect of the type of matrix employed on the delamination process under this fatigue fracture mode. Three composite materials were selected for this purpose. Two of the composites employ the same unidirectional AS4 carbon-fibre reinforcement, while the third uses unidirectional IM7 carbon-fibre reinforcement. Both types of fibre have similar strength characteristics. On the other hand, the three epoxy matrices that make up the composites are different: two of them, 8552 and MTM45-1, have the characteristic of enhanced toughness, while the third resin, 3506-1, has not been modified to achieve enhanced features.

2. Experimental procedure

All tests were carried out on an axial/torsional test device manufactured by walter + bai (LFV 50-T250-HH servo-hydraulic fatigue testing machine), with an axial load capacity of 100 kN and a torsional load capacity of 250 Nm.

All the specimens were tested after being previously dried in order to avoid any influence of environmental conditions on the test results. Once the desired drying level had been attained, the specimens were stored in a drier for no longer than 96 ± 6 h before testing.

2.1. Materials

The test programme was conducted on three different types of composites, all with an epoxy matrix and carbon-fibre reinforcement. The fibre employed in two of the composites was AS4, while IM7 fibre was used in the third. The properties of both types of fibre are similar and should not affect the results given the type of loading employed.

The first composite, known commercially as Hexply® AS/8552 RC34 AW196, is manufactured with a modified resin (8552) in order to enhance its mechanical properties, especially its fracture toughness.

The second material has an unmodified resin (3501-6) and is commercially known as Hexply® AS/3501-6 RC37 AW190.

Finally, the third composite, known commercially as ACG® MTM45-1/IM7-145 is a high performance, high toughness resin (MTM45-1). Table 1 shows the basic mechanical properties of the three composites. It should be noted that the third composite generally displayed the highest values.

Table 1 shows the main properties of the three resins and Table 2 presents the elastic moduli (E and G) and ultimate strengths (σ, τ) in the longitudinal direction of the fibres ("$_{11}$") and in the transverse direction ("$_{22}$") of the three materials under study.

The specimens used in the characterization of the analysed materials subjected to delamination under both static and fatigue mode III loading correspond to the scheme shown in Fig. 1. They had a straight rectangular cross-section of uniform thickness and width and were manufactured by stacking 56 plies (28/insert/28). A non-adhesive insert (15 μm-thick sheet of Tygavac RF-260-R) was placed in the mid-plane of the specimen to promote initial delamination. All specimens have be placed in the oven at 70 ± 5 °C for 96 ± 6 h after which the weight of the cores was recorded. Taking the previous weight as a reference, the specimens are put back into the oven, this time at 90 ± 5 °C and extracted every 24 ± 2 h, comparing the weight obtained with the immediately preceding one. Drying is completed when the difference between successive weighing is less than 0.5 mg per gram of sample. Once the exposed drying condition has been reached, the test pieces were stored in a desiccator.

During the test, in the laboratory, the temperature and relative humidity are practically constant and the possible moisture penetration would affect the three materials equally.

Although some of the parameters that define the elastic behaviour of the material are of the same order, others such as shear strength are clearly different; it must be considered that this is the parameter that can most affect the delamination phenomenon in mode III. In the case of material with IM7 reinforcement, it has a relative bad behaviour in static regime, however, in dynamic regime, the behaviour improves substantially so it can be deduced that it offers a greater resistance to the propagation of cracks to fatigue.

2.2. Test method

A specific test device was used to carry out the entire experimental programme. Fig. 2 shows a sketch of the test system used, by means of

Table 1
Properties of the three resins.

Epoxy resin	Density (g/cm^3)	Tensile modulus (GPa)	Tensile strength (MPa)	Tg onset dry (°C)
8552	1.316	4.67	121	200
3501-6	1.265	4.24	45.5	210
MTM45-1 [41]	1.18	3.35	120	180

Table 2
Mechanical properties of the three composites.

Material	Young's modulus (GPa)		Ultimate stresses (MPa)		Shear modulus (GPa)	Ultimate shear stress (MPa)
	E_{11}	E_{22}	σ_{11}	σ_{22}	G_{12}	τ_{max}
AS4/8552	144	10.6	1703	30.8	5.36	67.7
AS4/3501-6	131	8.9	1954	24	5.09	79.3
IM7/MTM45-1	174	12.6	2200	36.2	5.3	93.1

which the torque, M, generated on the upper jaw, which forms an integral part of the test device actuator, is transformed into a point load, P, parallel to the specimen's plane of delamination using a 2 mm-diameter roller. In the same Fig. 2, the specimen, the direction of the applied load and the nomenclature used in the most representative dimensions are schematically represented for both the static and cyclic fatigue fracture characterization of the three composites under study.

2.3. Static fracture toughness under mode III loading

The validity of the LHFB method in testing laminate composites under mode III fracture loading has been demonstrated in previous publications [33–35]. The formula presented below, based on the Timoshenko beam theory, in which cross-sectional warping is considered, was used to calculate the energy release rate:

$$G = \frac{1}{b}\left[\frac{P^2L^2}{2EI_z} + \frac{3P^2}{4bhG}\right]$$

where E and G are the elastic constants of the material, and I_z is the moment of inertia of the upper laminate with respect to the vertical axis. The meanings of the remaining terms are given in Fig. 1.

Prior static characterization tests of the materials under study were carried out maintaining the torsion angle on the test equipment at a speed of 0.01°/s and applying the load on the test piece at 10 mm from the crack front for materials AS4/8552 and AS4/3501-6, and at 1 mm for material MTM45-1/IM7-145 so as to minimize the possible effect of mode II fracture. In previous work [35] has been presented the components in modes I, II and III for two of the materials, observing that between 1 and 10 mm, the component in mode I is non-existent and the one in mode II is below 2.2%. The same trend was observed for IM7 so the decision of the point of application was taken based on the dynamic response of the test equipment.

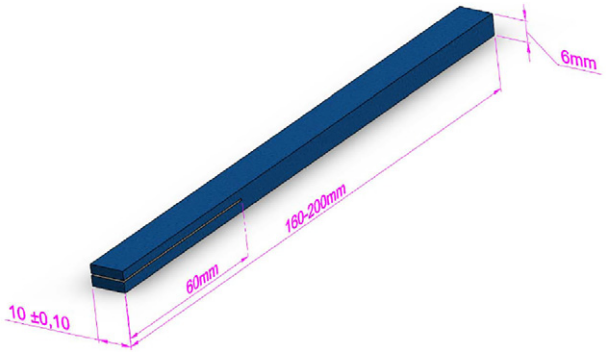

Fig. 1. Mode III fracture test specimen.

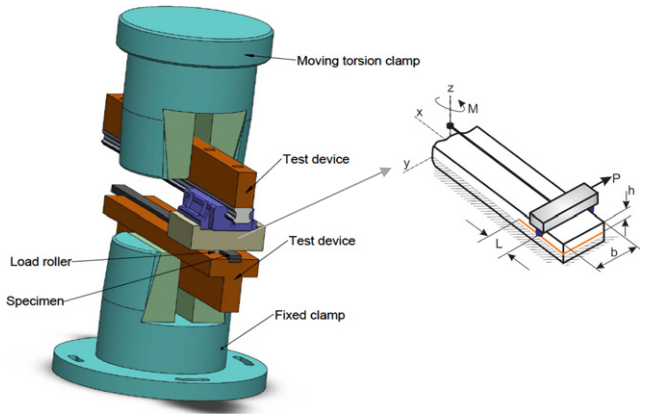

Fig. 2. Mode III fracture test device.

2.4. Cyclic fatigue fracture toughness under mode III loading

The aim of the experimental fatigue programme was to determine the fatigue curves of the tested material when subjected to fracture delamination processes under cyclic fatigue fracture mode III loading.

The same test device and machine as those used in the prior static characterization were used to perform the fatigue tests. This setup allowed a point load parallel to the plane of delamination to be applied to the tested specimens following a sine wave. Throughout the study, fatigue failure was considered to have commenced when complete delamination of the specimen had occurred. For this type of loading, the processes of onset of the crack and its subsequent growth occur almost simultaneously.

To conduct the proposed experimental study, the test strategy employed was that of applying constant levels of loading in combination with isolated trials. To define these levels, the results obtained from the prior characterization of the material under static loading were taken as a reference, calculating them as percentages of the critical energy release rate, G_c. All the fatigue tests were carried out by controlling the torque, M, applied to the specimens in the test device, employing an asymmetry coefficient of $R = 0.1$ and a constant frequency of 4 Hz throughout the entire test.

As stated previously, the fracture behaviour of the studied materials under mode III fatigue fracture loading was analysed only from the perspective of complete delamination of the specimen, as once delamination commenced, its subsequent propagation occurred immediately. That is to say, the crack progressed unstably under this fracture mode at practically all levels of loading. Hence, throughout the test, the distance of 1 mm between the point of application of the load and the crack front may be considered constant, based on the assumption that the crack grows instantaneously until complete delamination of the specimen.

Two million cycles were considered as the fatigue limit during all the fatigue tests and for all three materials, although in some of the materials this value occasionally exceeded 3 million cycles. Both these values were used as a reference for the choice of the aforementioned fatigue limit, the number of tested specimens per material being: 20 for AS4/8552, 16 for AS4/3501-6 and 22 for IM7/MTM45-1.

2.5. Statistical model used to evaluate the results

In order to improve the reliability of the evaluation of the results obtained in the experimental programme, a probabilistic analysis based on a Weibull regression model proposed by Castillo et al. [42,43] was carried out that allowed the normalization of the entire fatigue lifespan and which has already been shown to be effective in other cases involving composites [44]. This model allows us to obtain the entire fatigue life

field from a representative sample of experimental data.

$$P_f = F(N;G) = 1 - exp\left[\left(\frac{log(N/N_0)\cdot log(G_{max}/G_0) - \lambda}{\delta}\right)\right] \quad (3)$$

with $log(N/N_0)\cdot log(G_{max}/G_0) \geq \lambda$

where N is the fatigue life measured in cycles; G, the applied range of loading; P_f, the probability of failure; and G_0, N_0, β, λ and δ are the parameters to be estimated, with the following denotations:

N_0: threshold value or limit number of cycles

G_0: limiting fracture energy

β: shape parameter of the Weibull distribution

λ: a parameter that sets the position of the limit curve or the null probability.

δ: scale parameter.

3. Experimental results and discussion

The experimental results are presented below.

3.1. Static behaviour

Table 3 presents the mode III fracture toughness for the three materials calculated from the expression given above and deduced from Timoshenko's beam theory and an average of five tests carried out for each material.

It can be seen that the composite manufactured with the MTM45-1 resin, which presented the best mechanical properties in Table 2 and was assumed to be tough, is the one that yields the lowest ERR value. The next lowest value is that of resin 8552, also assumed to be tough, while the highest value is that presented by the supposedly more fragile resin. In previous research [39] studying only the two composites containing AS4 fibre, the static values under mode I fracture were found to be higher for the composite manufactured with resin 8552, while for mode II fracture, the highest ERR value was obtained with resin 3501-6.

3.2. Cyclic fatigue fracture behaviour

Fig. 3 shows the experimental results of all the specimens of all three types of tested materials, together with the line fittings for each of the specimens.

A less steep slope is observed in the fitting of the results obtained in material AS4/3501-6, which indicates a lower loss of fatigue properties of the material during its fatigue lifespan. However, this material is clearly observed to be the one with the greatest loss in strength with respect to the results obtained under static loading, given that the maximum level of loading reached in the low number of cycles is 29% that obtained under static loading and 18% in the infinite lifespan zone.

The behaviour of the other two materials, which in principle have a tougher matrix, can be considered better in the low number of cycles zone from the point of view of their loss of strength, taking as reference their capacity under static loading. The material manufactured with the 8552 matrix reaches fatigue loading levels of 42% of that reached under static loading, while the material manufactured with the MTM45-1 matrix reaches levels of 47%. As to the fatigue limit achieved in these two materials, AS4/8552 and IM7/MTM45-1, their behaviour is substantially

Table 3
Static values of the energy release rate for the three materials.

	AS4/8552	AS4/3501-6	IM7/MTM45-1
G_{III} (J/m^2)	796	956	720
Standard deviation	49	78	110
Dev. %	5.8	8.7	15.3

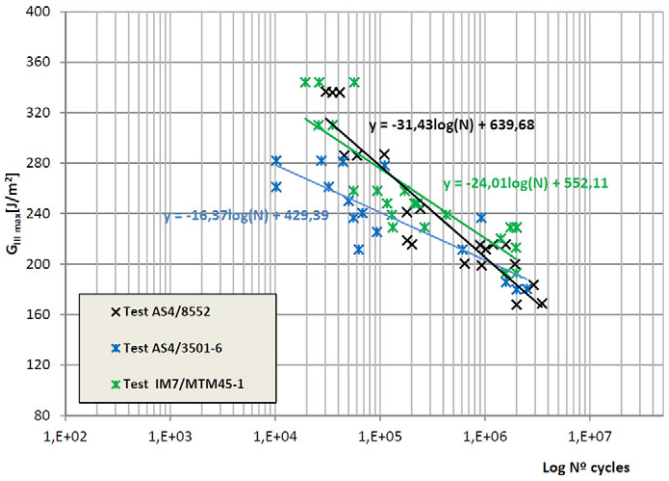

Fig. 3. Results of all tests performed for all three materials at different percentages of the maximum torque.

different. The 8552 matrix is the one with the lower fatigue limit of 20% of the energy release rate achieved under static loading compared to 27% in the MTM45-1 matrix.

To achieve a better understanding of the results of experimental fatigue programmes, it is generally convenient to carry out a statistical standardization that allows comparing the results thus obtained with certain criteria. Fig. 4 accordingly shows the percentile curves for a 5% probability of failure for the three tested materials. Similarly, the percentile curves for a 50% probability of failure for the three tested materials are represented in Fig. 5. From the analysis of both figures, it can clearly be seen that the fatigue behaviour of the material manufactured with the 3501-6 matrix is clearly inferior to that of the other two materials, which, in turn, behave quite similarly.

This result can be justified taking into account the characteristics of the matrices used, as both 8552 and MTM45-1 are known to be tough matrices, which is not the case with 3501-6. It should be noted that this trend observed during the fatigue characterization of these materials is contrary to that observed under static loading, the values for which were previously presented in Table 2.

On the contrary, just as in the static case, previous fatigue studies carried out with two of the materials, AS4/8552 and AS4/3501-6, the former was shown to perform better under cyclic fatigue mode I fracture loading, but worse under mode II loading.

The fatigues limit for both of the reported probabilities of failure and this fracture mode of fracture is practically the same in the two materials respectively manufactured with the 8552 and 3501-6 matrices, while that corresponding to the material manufactured with the MTM45-1 matrix has an approximately 10% higher fatigue limit, in the

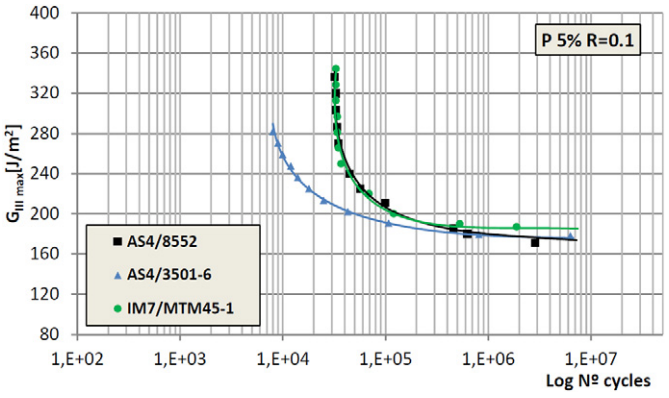

Fig. 4. 5% percentile curves for the three materials.

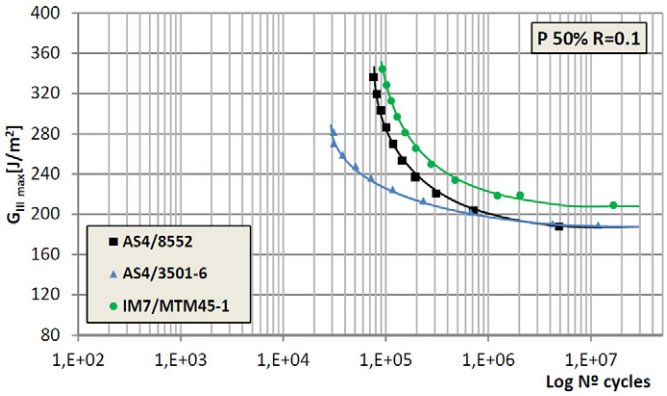

Fig. 5. 50% percentile curves for the three materials.

case of taking the maximum energy release rate achieved in fatigue tests as a reference.

4. Fractographic analysis

Different studies have shown SEM fractography to be an important complement in the fracture analysis of composites given the high number of fracture mechanisms that coexist in materials of this kind [45].

The analysed specimens, which were obtained in all cases from fatigue tested specimens, were taken from the region of the crack, near the insert, as this is the most significant area to carry out this study. Several regions close to the insert obtained for the 8552 material with different fractographs are shown in Figs. 6–8.

In Fig. 6, corresponding to the 8552 matrix, the presence of a considerable number of broken fibres that are the end result of the fracture of the possible fibre bridges that had been formed and which afford a major toughness value to this material can be appreciated in this region. The existence of fibre bridges in mode III fracture in laminated composites is worth emphasizing due to the fact that, until now, this appeared to be a phenomenon that only existed in mode I fracture [16].

In Fig. 7, corresponding to the 8552 matrix, the presence of a typical mode III phenomenon can be observed, i.e. beds of resin caused by the friction of one face of the specimen on the other. Finally, another typical mode III fractography can be observed in Fig. 8 that has been previously detected in specimens that underwent static fracture, i.e. the presence of flakes located at an angle of 45° to the axis of the fibres due to the fact that the stress state is dominated by tangential stresses in the direction of the fibres and perpendicular to their direction. Given this stress

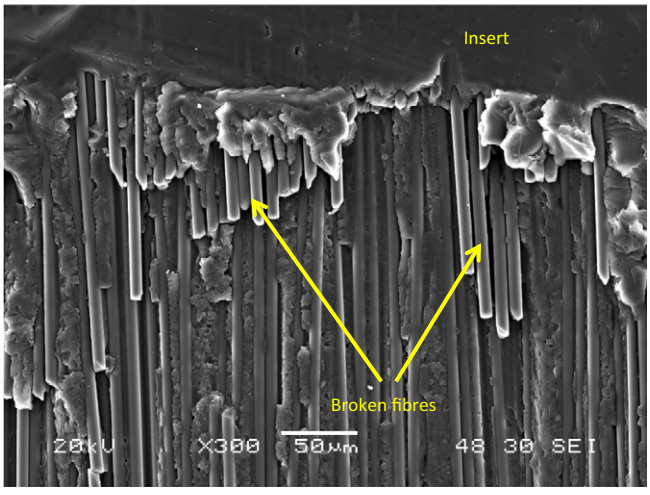

Fig. 6. Micrograph of material AS4/8552 in a region near the insert where a substantial number of broken fibres can be appreciated.

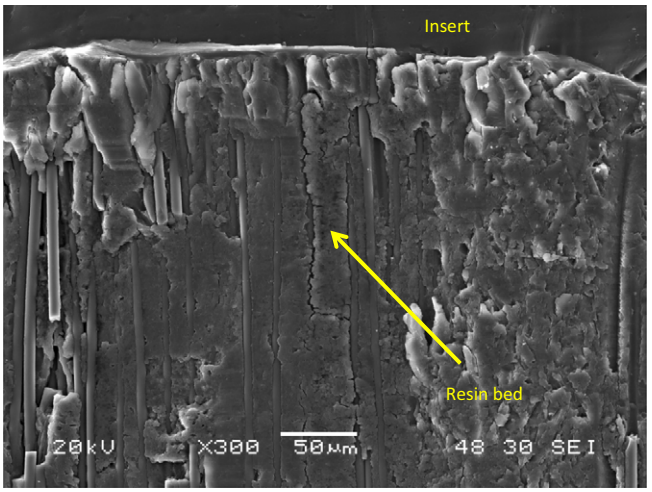

Fig. 7. Micrograph of material AS4/8552 in a region near the insert where resin beds can be appreciated.

state, the main stresses will be oriented in the bisector of the angle formed by the aforementioned directions. These main stresses produce fracture in the planes located at 45°, which justifies the observed morphology. In some cases, these flakes end up presenting a morphology previously given the name 'sawteeth'.

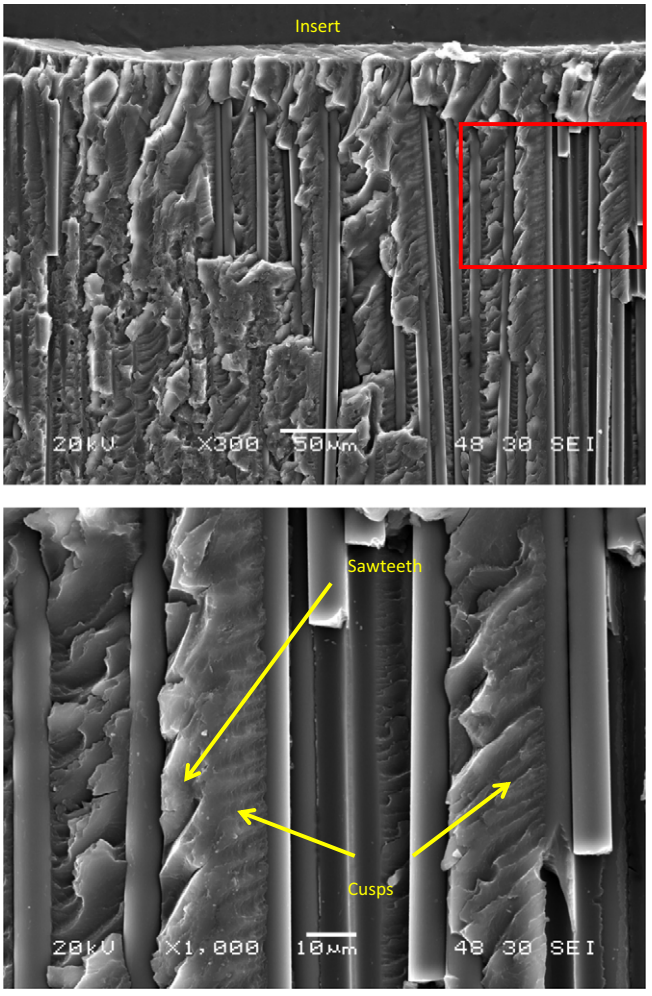

Fig. 8. Micrograph of material AS4/8552 in a region near the insert where different morphologies can be appreciated.

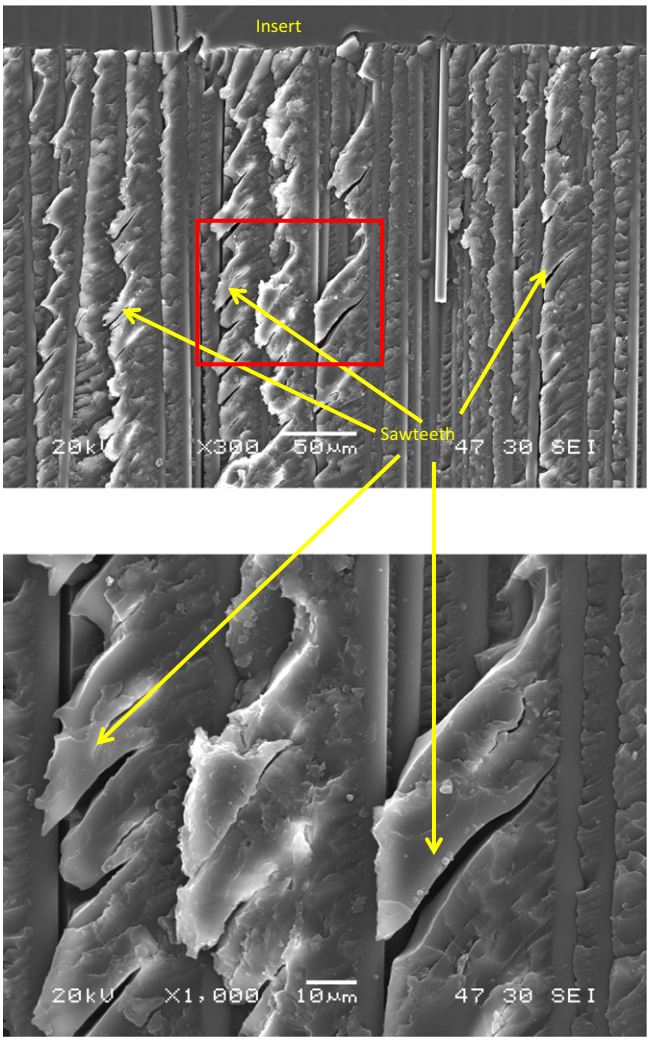

Fig. 9. Micrograph of material AS4/3501-6 in a region near the insert where a morphology in which sawteeth are predominant can be appreciated.

In Fig. 9, corresponding to material AS4/3501-6, the typical morphology of a composite with a fragile matrix can clearly be observed, with pronounced sawteeth likewise oriented at an angle of 45°, very few broken fibres and the absence of the aforementioned resin beds.

Finally, fractographs of material IM7/MTM45-1 are presented in Figs. 10 and 11. The differences with respect to the previous figures are clear. Large resin beds are formed that subsequently break up, exposing areas of clean fibres with small flakes between them. Broken fibres are practically undetected and the small flakes do not present a preferred orientation.

In summary, for material AS4/8552, morphologies are produced that point to an increase in toughness, such as broken fibres and resin beds, and others that indicate fragility, namely flakes and sawteeth at 45°. Material AS4/3501-6 only presents the latter morphology; hence its low ERR values. Finally, material IM7/MTM45-1 mostly presents a morphology with resin beds, which, as previously stated, is characteristic of tough materials subjected to this fracture mode.

5. Conclusions

The Longitudinal Half Fixed Beam (LHFB) device is valid for obtaining the values of both static and cyclic fatigue ERR for laminated composite materials regardless of the type of resin that constitutes its matrix.

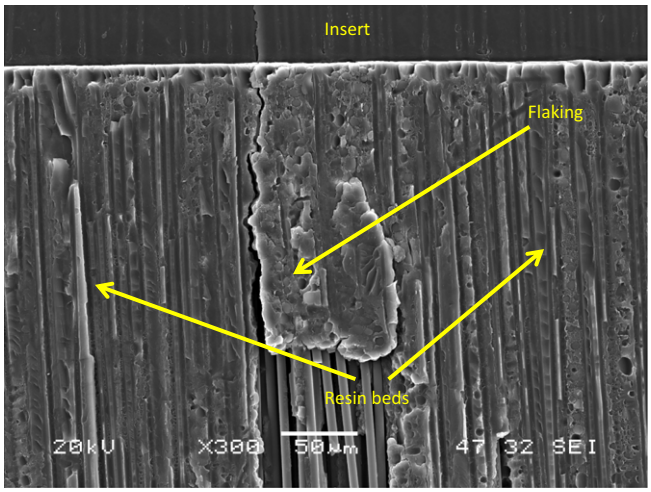

Fig. 10. Resin bed with flaking.

A composite material with high mechanical properties (modulus, strength, etc.) does not have to have high fracture toughness. Likewise, a composite laminate may have a higher ERR than another composite in one fracture mode and a lower value in another. Although the ERR value in these types of materials effectively depends on the resin that constitutes its matrix, its behaviour varies depending on the type of stress to which it is subjected.

In trials of this type, the results should be treated statistically so that they can be analysed more clearly in both the low and high number of cycles zone. In the present study, one of the materials presents tough behaviour at a low number of cycles and more fragile behaviour at a high number of cycles.

In materials of this type, fractography is an irrefutable proof of the fracture mechanism that occurs. This study presents three principal morphologies. The first, consisting of broken fibres, was typical of mode I fracture and non-existent in mode II fracture. It did not seem very predictable in mode III fracture, although it was present to a significant degree in one of the materials. This morphology is representative of toughness. The second comprises cusps, which may or may not finally form sawteeth, all of which present a preferred orientation at 45°. These are typical of mode III fracture in materials with a fragile matrix subjected to this loading mode. Moreover, the more fragile the matrix, the greater the number of sawteeth that appear. Finally, the third morphology is made up of beds of resin. In this case, the matrix is not fragile and

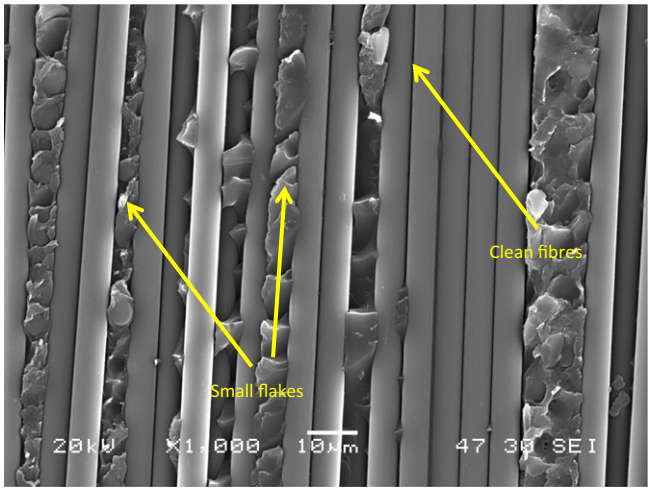

Fig. 11. Morphology after flaking with the presence of clean fibres and small flakes.

does not break (cusps or sawteeth), but in fact stretches. Subsequently, when the direction of movement changes, blocks of resin are formed that end up cracking and flaking. This is proof of the high toughness of the matrix.

Declaration of competing interest

The authors declare that they have no known competing financial interests or personal relationships that could have appeared to influence the work reported in this paper.

Acknowledgments

The authors are indebted to the Spanish Ministerio de Ciencia, Innovación y Universidades (Project RTI2018-095290-B-I00) for funding this study.

References

[1] J.R. Gregory, S. Spearing, Delamination initiation predictions from constituent behavior, 14th International Conference of Composite Materials, San Diego, CA, 2003.
[2] T.K. O'Brien, Characterization of delamination onset and growth in a composite laminate, in: K.L. Reifsnider (Ed.), Damage in Composite Materials, 775, ASTM STP, Philadelphia 1982, pp. 140–167.
[3] M. Hojo, S. Matsuda, M. Tanaka, C. Göran Gustafson, R. Hayashi, Effect of stress ratio of near-threshold propagation of delamination fatigue cracks in unidirectional CFRP, Compos. Sci. Technol. 29 (1987) 273–292.
[4] U. Hansen, J.W. Gillespie, Dependence of intralaminar fracture toughness on direction of crack propagation in unidirectional composites, Journal of Composites Technology & Research 20 (1998) 89–99.
[5] K. Paul, L. Kelly, V. Venkayya, T. Hess, Evolution of US military aircraft structures technology, J. Aircr. 39 (2002) 18–29.
[6] M. Rayandi, W.S. Teo, L.Q.N. Tran, M.S. Yong, T.E. Tay, The effects of through-the-thickness stitching on the mode I interlaminar fracture toughness of flax/epoxy composite laminates, Mater. Des. 109 (2016) 659–669.
[7] A. Szekrényes, J. Uj, Over-leg bending test for mixed-mode I/II interlaminar fracture in composite laminates, International Journal of Damage Mechanics 16 (2007) 5–33.
[8] D. Quan, J. Labarga, A. Ivankovic, Enhancing mode-I and mode-II fracture toughness of epoxy and carbon fibre reinforced composites using multi-walled carbon nanotubes, Mater. Des. 143 (2018) 81–92.
[9] H. Yoshihara, Mode II fracture mechanics properties of wood measured by the asymmetric four-point bending test using a single-edge notched specimen, Eng. Fract. Mech. 75 (2008) 4727–4739.
[10] Q. Chen, C. Dai, C. Fang, M. Chen, B. Fei, Mode I interlaminar fracture toughness behaviour and mechanisms of bamboo, Mater. Des. 183 (2019), 108132.
[11] S. Stelzer, A.J. Brunner, A. Argüelles, N. Murphy, G. Pinter, Mode I delamination fatigue crack growth in unidirectional fiber reinforced composites: development of a standardized test procedure, Compos. Sci. Technol. 72 (2012) 1102–1107.
[12] S. Stutz, J. Cugnoni, J. Botsis, Studies of mode I delamination in monotonic and fatigue loading using FBG wavelength multiplexing and numerical analysis, Compos. Sci. Technol. 71 (2011) 443–449.
[13] V. Danodaran, A.G. Castellanos, M. Milostan, P. Prabhakar, Improving the mode-II interlaminar fracture toughness of polymeric matrix composites through additive manufacturing, Mater. Des. 157 (2018) 60–73.
[14] A. Argüelles, J. Viña, A. F. Canteli, J. Bonhomme, Influence of resin type on the delamination behavior of carbon fibre reinforced composites under mode-II loading, International Journal of Damage Mechanics 20 (2011) 963–978.
[15] A. Argüelles, P. Coronado, A. F. Canteli, J. Viña, J. Bonhomme, Using a statistical model for the analysis of the influence of the type of matrix carbon-epoxy composites on the fatigue delamination under modes I and II of fracture, Int. J. Fatigue 56 (2013) 54–59.
[16] Chen Q, Dai, C, Fang C, Chen M, Zhang S, Liu R, Liu X, Fei, B, Mode I interlaminar fracture toughness behaviour and mechanisms of bamboo, Mater. Des., doi: https://doi.org/10.1016/j.matdes.2019.108132.
[17] D. Broek, Elementary Engineering Fracture Mechanics, 4th edition Kluwer Academic Publishers Group, 1986.
[18] M. Hrstka, S. Zak, T. Vojtek, Large plastic zones and extensive influence of notch under near-threshold mode II and mode III loading of fatigue cracks, Procedia Structural Integrity 13 (2018) 1123–1128.
[19] M. Salviato, M. Zappalorto, L. Maragoni, Exact solution for the mode III stress fields ahead of cracks initiated at sharp notch tips, European Journal of Mechanics-A/Solids 72 (2018) 88–96.
[20] S.L. Donaldson, Mode III Interlaminar fracture characterization of composite materials, Compos. Sci. Technol. 32 (1988) 225–249.
[21] S.F. Hwang, C.L. Hu, Tearing mode interlaminar fracture toughness of composite materials, Polym. Compos. 22 (1) (2001) 57–64.
[22] N.K. Naik, K.S. Reddy, S. Meduri, N.B. Raju, P.D. Prasad, S.K.N.M. Azad, P.A. Ogde, B.C.K. Reddy, Interlaminar fracture characterization for plain weave fabric composites, J. Mater. Sci. 37 (2002) 2983–2987.
[23] F. Sharif, M.T. Kortschot, R.H. Martin, Mode III delamination using a split cantilever beam, in: R.H. Martin (Ed.), Composite Materials Fatigue and Fracture- Fifth Volume, ASTM STP 1230, American Society for Testing and Materials, Philadelphia 1995, pp. 85–99.
[24] A. Szekrényes, Improved analysis of the modified split-cantilever beam for mode III fracture, Int. J. Mech. Sci. 51 (2009) 682–693.
[25] J. Li, S.M. Lee, E.W. Lee, T.K. O'Brien, Evaluation of the edge crack torsion test (ECT) for mode III interlaminar fracture toughness of laminated composites, J. Compos. Technol. Res. 19 (1997) 174–183.
[26] W.C. Liao, C.T. Sun, The delamination of mode III fracture toughness in thick composite laminates, Compos. Sci. Technol. 56 (1996) 489–499.
[27] D. Pennas, W.J. Cantwell, P. Compston, The influence of strain rate on the mode III interlaminar fracture of composite materials, J. Compos. Mater. 41 (2007) 2595–2614.
[28] A.B. Morais, A.B. Pereira, M.F.S.F. de Moura, A.G. Magalhaes, Mode III interlaminar fracture of carbon/epoxy laminates using the edge crack torsion (ECT) test, Compos. Sci. Technol. 69 (2009) 670–676.
[29] M. de Moura, M. Fernandez, A. de Morais, R. Campilho, Numerical analysis of the edge crack torsion test for mode III interlaminar fracture of composite laminates, Eng. Fract. Mech. 76 (2009) 469–478.
[30] D. Pennas, W. Cantwell, The influence of loading rate on the mode III interlaminar fracture toughness of composite/steel bi-material systems, J. Compos. Mater. 43 (2009) 2255–2268.
[31] Y. Ge, X. Gong, A. Hurez, E. de Luycker, Test methods for measuring pure mode III delamination toughness of composite, Polym. Test. 55 (2016) 261–268.
[32] M.W. Czabaj, J.G. Ratcliffe, B.D. Davidson, Observation of intralaminar cracking in the edge crack torsion specimen, Eng. Fract. Mech. 120 (2014) 1–14.
[33] H. Yoshihara, Examination of the 4-ENF test for measuring the mode III R-curve of wood, Eng. Fract. Mech. 73 (2006) 42–63.
[34] A. Pereira, A. de Morais, M. de Moura, Design and analysis of a new six-point edge crack torsion (6ECT) specimen for mode III interlaminar fracture characterization, Composites Part A 42 (2011) 131–139.
[35] A. de Morais, A. Pereira, M. de Moura, Mode III interlaminar fracture of carbon/epoxy laminates using the six-point edge crack torsion (6ECT), Composites Part A 42 (2011) 1793–1799.
[36] B.D. Davidson, F.O. Sediles, Mixed-mode I-II-III delamination toughness determination via a shear-torsion-bending test, Composites Part A 42 (2011) 589–603.
[37] A.L. Johnston, B.D. Davidson, Intrinsic coupling of near-tip matrix crack formation to mode III delamination advance in laminated polymeric matrix composites, Int. J. Solids Struct. 51 (2014) 2360–2369.
[38] A. López-Menéndez, J. Viña, A. Argüelles, M. Lozano, Validation of the longitudinal half fixed beam method for characterizing mode III delamination of composite laminates, Compos. Struct. 147 (2016) 74–81.
[39] A. López-Menéndez, J. Viña, A. Argüelles, S. Rubiera, V. Mollón, A new method for testing composite materials under mode III fracture, J. Compos. Mater. 50 (28) (2016) 3973–3980.
[40] A. López-Menéndez, J. Viña, A. Argüelles, I. Viña, S. Rubiera, Analysis of mode III interlaminar fracture toughness of laminated composites using a novel testing device, Eng. Fract. Mech. 173 (2017) 55–63.
[41] A.S. Kaddour, M.J. Hinton, P.A. Smith, S. Li, Mechanical properties and details of composite laminates for the test cases used in the third world-wide failure exercise, J. Compos. Mater. 47 (2013) 2427–2442.
[42] E. Castillo, A. Fernández-Canteli, A general regression model for lifetime evaluation and prediction, Int. J. Fatigue 107 (2001) 117–137.
[43] E. Castillo, A. Fernández-Canteli, H. Pinto, M. López-Aenlle, A general regression model for statistical analysis of strain life fatigue data, Mater. Lett. 62 (2008) 3639–3642.
[44] A. Argüelles, P. Coronado, A. F. Canteli, J. Viña, J. Bonhomme, Using a statistical model for the analysis of the influence of the type of matrix carbon-epoxy composites on the fatigue delamination under modes I and II of fracture, Int. J. Fatigue 56 (2013) 54–59.
[45] J. Bonhomme, J. Viña, A. Argüelles, I. Viña, V. Mollón, Influence of the matrix toughness in carbon-epoxy composites subjected to delamination under modes I, II and mixed I/II, Mech. Adv. Mater. Struct. 20 (2013) 679–686.